# Supplementary Information

To further confirm that the desired $Ti_3C_2T_x$ had been obtained, the Fourier transform infrared (FTIR) spectra of the MAX and pure MXene specimens were recorded. As shown in Fig. S1b, peaks were observed at 1621, 1041, 1114, and 1444 cm^{-1}, which correspond to the C=O, C–O, C–F, and O–H vibrations, respectively. In addition, the stretching band at 3500 cm^{-1} can be indexed to the OH vibration of water. After ultrasonic exfoliation, the surfaces of the $Ti_3C_2T_x$ nanosheets retained the original abundance of functional groups.

Transmission electron microscopy (TEM) was then used to further investigate the microstructures of the products. The representative TEM image shown in Fig. S1c indicates that $Ti_3C_2T_x$ was composed of a layered structure after etching of the Al layers. In addition, the field of view is composed of a large number of extremely thin nanosheets (with radial dimensions of several hundred nanometers to several micrometers), which form a stacked structure with bent or folded edges.
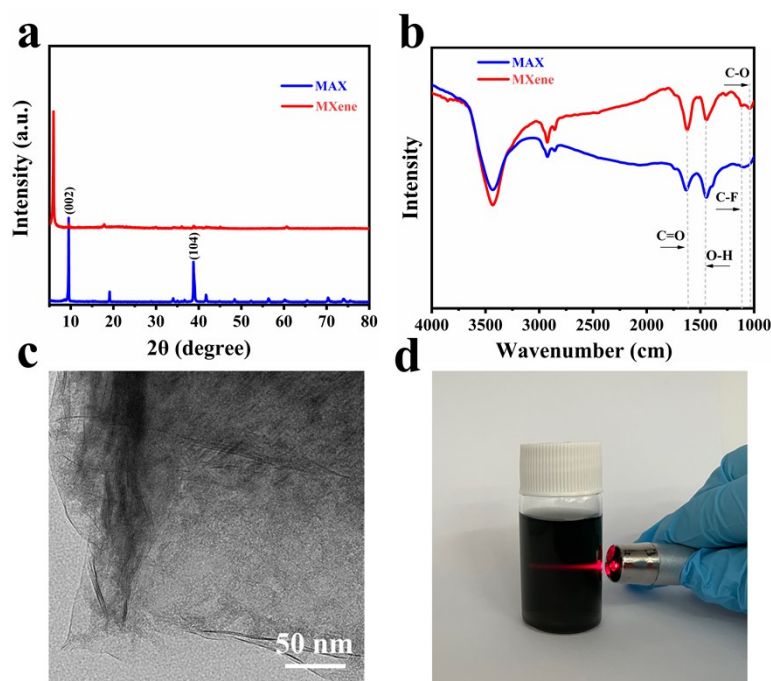

Fig. S1 (a) XRD and (b) FT-IR results for the MAX and pure MXene powders. (c) TEM image of the MXene powder. (d) The Tyndall effect of the MXene suspension.

Fig. S2 shows the infrared spectrum of $K_6[P_2W_{18}O_{62}]\textcircled{1}14H_2O$, wherein the broad peak at 3432 cm^{-1} corresponds to the water molecules. In addition, four absorption peaks were observed at 597–1100 cm^{-1}, and these can be attributed to the characteristic absorption peaks of the P–O_a, W–O_d, W–O_b–W, and W–O_c–W stretching vibrations in the 2:18 series Dawson-type heteropolyanion skeleton of $[P_2W_{18}O_{62}]^{6-}$.
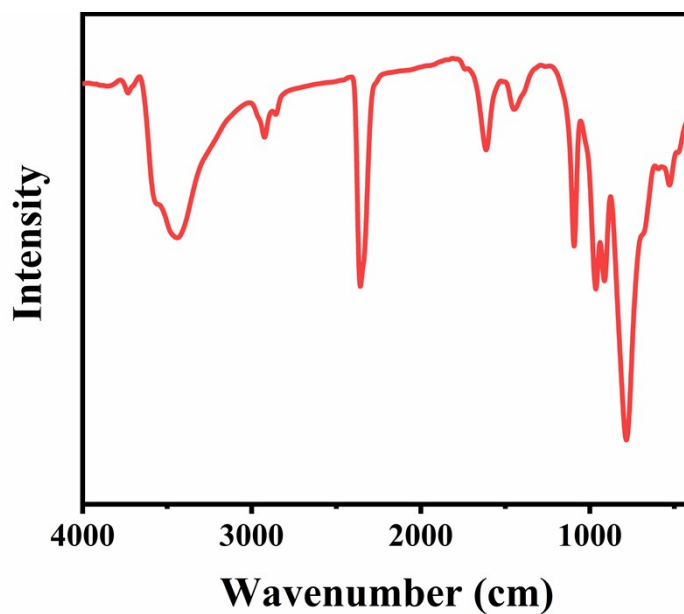

Fig. S2 FT-IR spectrum of P_2W_{18}.

Growth of the composite film was monitored by UV-vis spectroscopy. As shown in Fig. S3, the absorption peak at 202 nm can be attributed to POMs, while that at 754 nm originated from $Ti_3C_2T_x$. The obtained results suggest that the $NW@MXene/P_2W_{18}$ film grew in an orderly manner as the number of layers increased, thereby indicating that uniform growth was achieved during each deposition cycle.
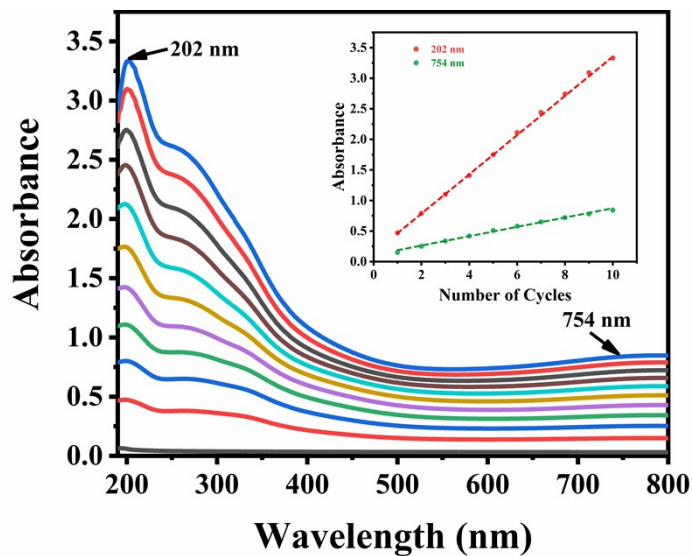
Fig. S3 UV-vis absorption spectra recorded during growth of the composite film on a quartz substrate over 0-10 cycles.

Two-dimensional and three-dimensional images of the MXene/P_2W_{18} composite films are shown in Figs. S4a and S4b. Based on an area of 5×5 μm^2 in the AFM image, the mean square roughness of the MXene/P_2W_{18} composite film was determined to be 34.4 nm.
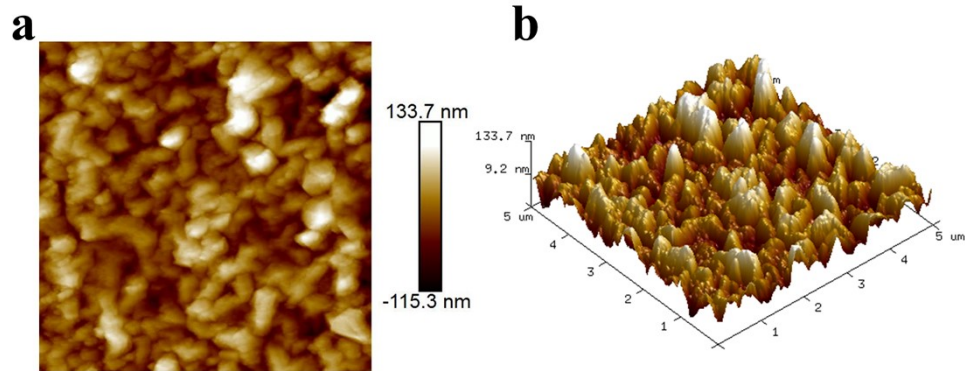
Fig. S4 (a) 2D and (b) 3D AFM images of the MXene/P_2W_{18} film.
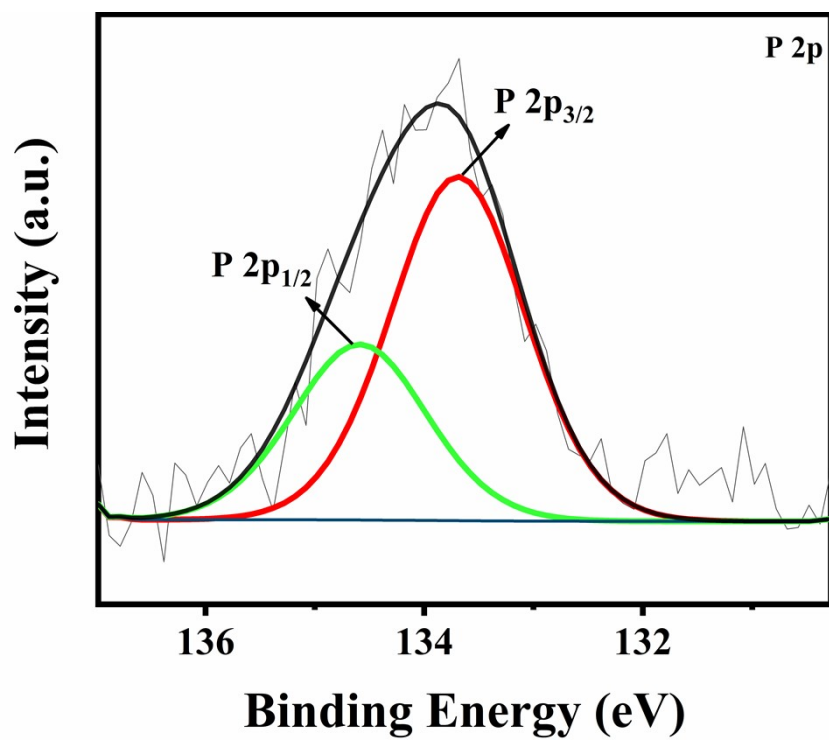
Fig. S5 XPS results: P 2p spectra recorded for the NW@MXene/P$_2$W$_{18}$ film.

The surface coverage of the film was calculated using Equation S1, wherein I_p, n, v, A, and Γ_0 represent the peak current (A), the electron number, the scan rate (V s^{-1}), the electrode surface area (cm^2), and the surface coverage (mol cm^{-2}), respectively. The diffusion coefficient (D) of the active material was obtained using the Randles–Sevcik equation (Equation S2), wherein C_0 represents the concentration of the active ions in the solution (mol L^{-1}).

$$I_p = \frac{n^2 F^2 v A \Gamma_0}{4RT} \quad \text{(S1)}$$

$$D^{1/2} = \frac{\dfrac{I_p}{A}}{2.72 \times 10^5 \times n^{3/2} \times A \times C_0 \times v^{1/2}} \quad \text{(S2)}$$

Table S1. Values of various parameters involved in EIS

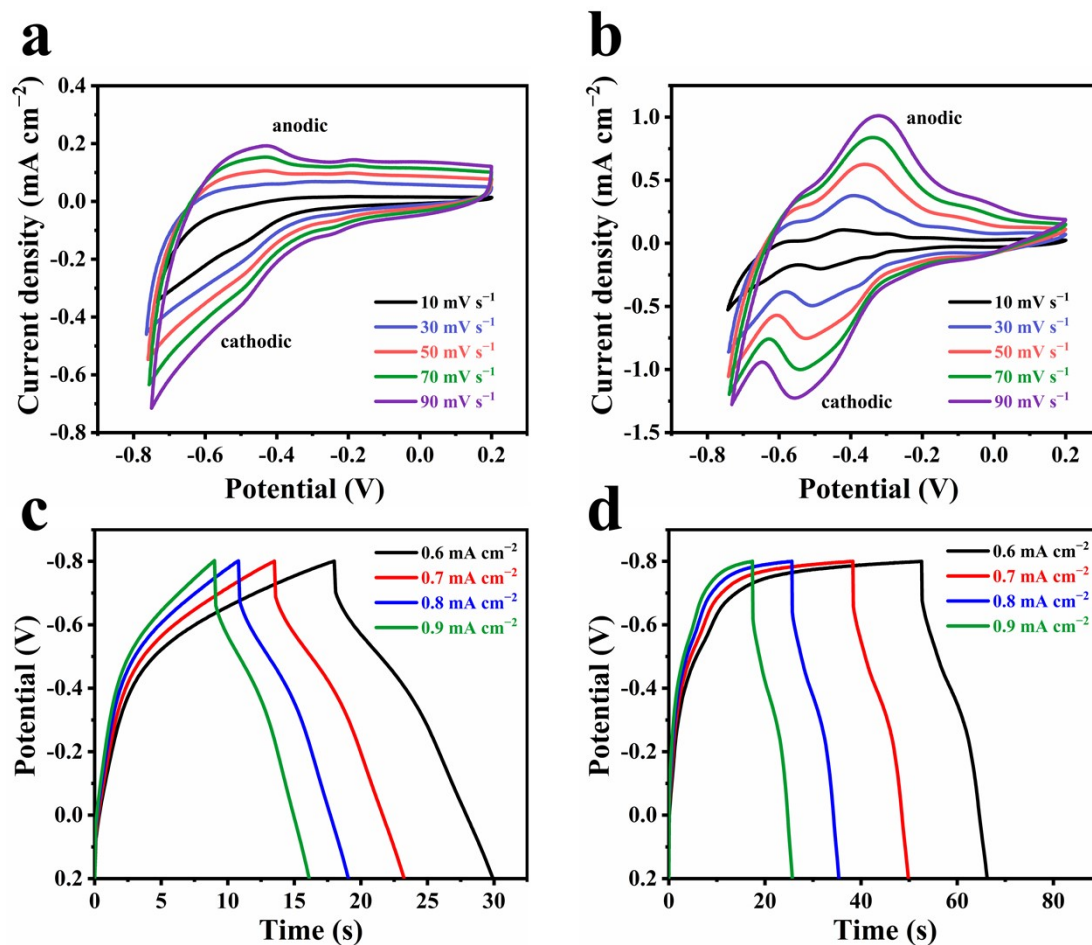| Name of the material	Equivalent series resistance (R_s)	Charge transfer resistance (R_{ct})	Warburg impedance (W)
MXene/P$_2$W$_{18}$	16.73 Ω	70.84 Ω	3.24 KΩ
NW@MXene/P$_2$W$_{18}$	17.22 Ω	66.68 Ω	2.04 KΩ

Fig. S6 CV curves of the (a) MXene and (b) MXene/P$_2$W$_{18}$ films under different scan rates. GCD curves of the (c) MXene and (d) MXene/P$_2$W$_{18}$ films under various current densities.
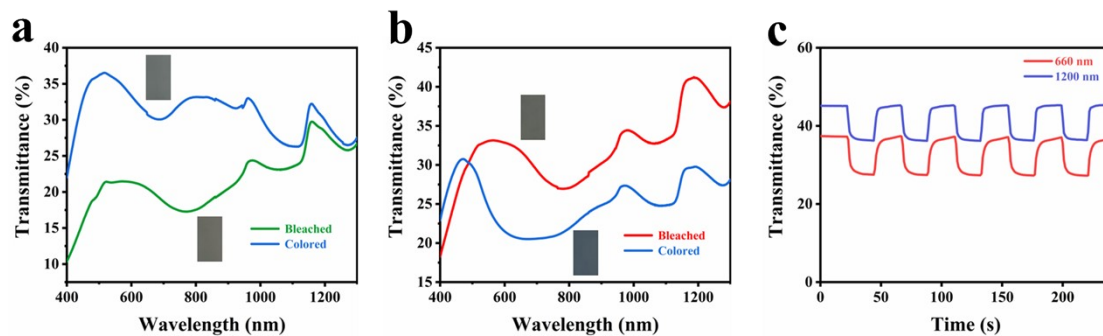
Equations used to calculate the Areal capacitance (C_{areal}), the energy density (E), and the power density (P):

$$C_{areal,\,GCD} = (i\Delta t)/(A\Delta V) \qquad \text{(S3)}$$

$$E = C_{areal,\,GCD}\Delta V^2/7200 \qquad \text{(S4)}$$

$$P = 3600E/\Delta t \qquad \text{(S5)}$$

where ΔV is the potential window, A is the area of the SC electrodes, i is the applied current, and Δt is the discharge time.

Fig. S7 Transmission spectra of the (a) MXene and (b) MXene/P_2W_{18} films in their bleached and colored states. (c) Transmission changes for the MXene/P_2W_{18} film at 660 and 1200 nm during the electrochromic process.
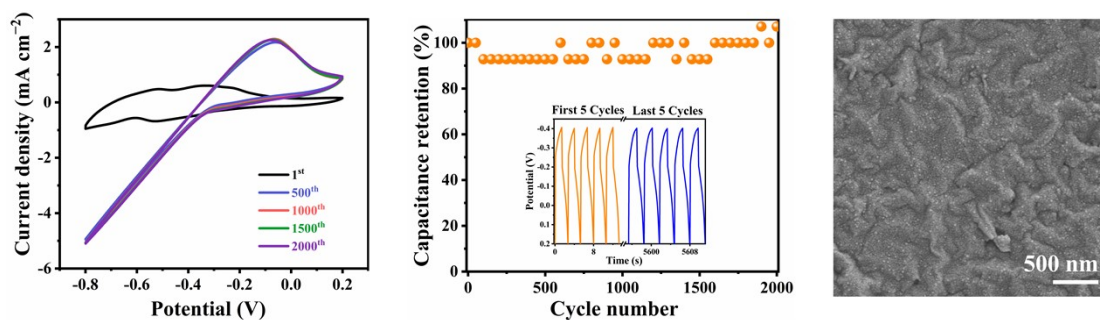
Fig. S8 (a) Comparison of CV curves before and after 2000 cycles (50 mV s^{-1}). (b) Long-term cycle test at 0.8 mA cm^{-2}. The illustration is the first and last of the five cycles of the GCD curve. (c) SEM image of MXene/P$_2$W$_{18}$ film after 2000 GCD cycles.
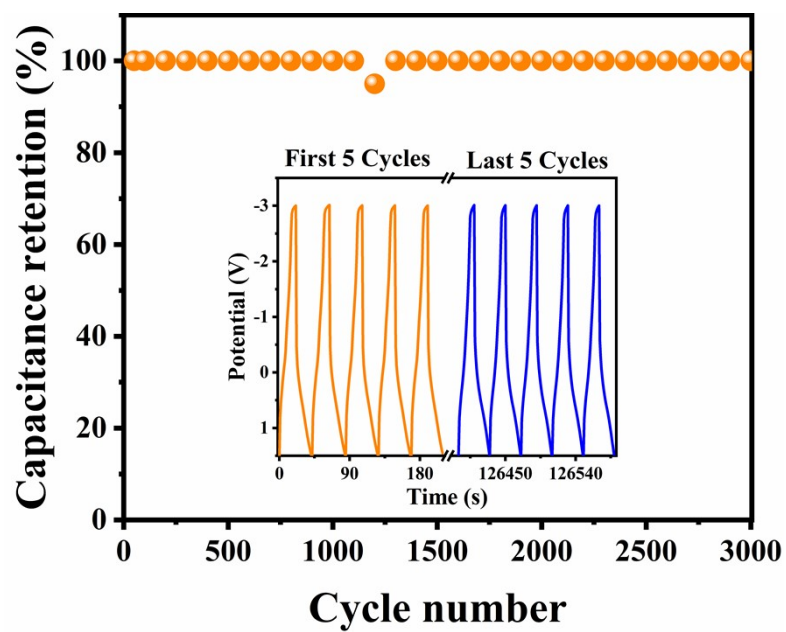
Fig. S9 Cycling performance of the ECSC at 0.18 mA cm^{-2}. The illustration is the first and last of the five cycles of the GCD curve.